science, engineering and health studies

Research Article

Science, Engineering and Health Studies
https://lio1.tci-thaijo.org/index.php/sehs
ISSN (Online): 2630-0087

4-Bromo-N,N-dimethylaniline, 4-fluoro-N,N-dimethylaniline, 4-methyl-N,N-dimethylaniline: Density-functional theory study

Hayat EL Ouafy[1], Mouna Aamor[1], Mustapha Oubenali[1], Mohamed Mbarki[1], Ahmed Gamouh[1], Aziz EL Haimouti[2] and Tarik EL Ouafy[2]*

[1] Department of Chemistry and Environment, Faculty of Sciences and Technics, Sultan Moulay Slimane University, Beni Mellal 23000, Morocco
[2] Department of Physics and Chemistry, Polydisciplinary Faculty of Khouribga, Sultan Moulay Slimane University, Beni Mellal 23000, Morocco

ABSTRACT

Classical physics perfectly describes our daily environment but becomes inoperative at the microscopic scale of atoms and particles. Quantum mechanics is then used, in which the quantities of matter or energy exchanged can no longer take any value and only discretes values. The present work studied the molecules of 4-bromo-N,N-dimethylaniline, 4-fluoro-N,N-dimethylaniline, 4-methyl-N,N-dimethylaniline by a very precise method, and the Density-functional theory (DFT) gave an important theoretical framework for deriving properties of quantum chemistry. The number of local reactivity descriptors based on DFT containing electron density was given to facilitate the understanding of the reactivity of atoms and to determine the ionization potential, electronic affinity, chemical hardness, electronegativity and overall softness, maximum charge transfer, overall electrophilicity, as determined by using nonlinear optical descriptors. To prove the stability of the molecules, the 3D maps of the highest occupied moleculars orbit, the lowest unoccupied molecular orbit, and the Mulliken charges of each molecule was determined. The electrostatic potential served as a guide for the early stages of a reaction, in which the interacting species were not yet very close to each other, the bond lengths and angles of our molecules.

Keywords: DFT; chemical descriptor; nonlinear optical descriptors; electrostatic molecular potential; density-functional theory

***Corresponding author**:*
Tarik EL Ouafy
tarikelouafy@gmail.com

***Received**: 23 November 2020*
***Revised**: 15 February 2021*
***Accepted**: 19 February 2021*
***Published**: 28 December 2021*

***Citation**:*
EL Ouafy, H., Aamor, M., Oubenali, M., Mbarki, M., Gamouh, A., EL Haimouti, A., and EL Ouafy, T. (2021). 4-Bromo-N,N-dimethylaniline, 4-fluoro-N,N-dimethylaniline, 4-methyl-N,N-dimethylaniline: Density-functional theory study. Science, Engineering and Health Studies, 15, 21020012.

1. INTRODUCTION

In recent years, hybrid compounds based on metal halides have the advantages of organic and inorganic compounds. These compounds are usually marked by their structural and their interest in properties such as non-linear optical activity, magnetic and catalytic properties (Wojtaś et al., 2009; Han et al., 2005). Dimethylaniline (DMA) is an aromatic compound with the formula $C_8H_{11}N$. It consists of one molecule of aniline (aminobenzene), substituted by two methyl groups. By habit, the term "dimethylaniline" is rather reserved for derivatives where at least one of the methyl groups is carried by the amine group, and in particular, the term is often even associated with the single isomer where the two methyl groups are carried by the amine group, N,N-dimethylaniline. $C_8H_{10}BrN$ has been determined from iodide in pharmaceuticals and organic compounds in vegetables and milk (Pardo et al., 2011).

Organic materials have been used for many purposes, especially for molecular electronics. The halogens of aniline are 4-Bromo-N,N-dimethylaniline $C_8H_{10}BrN$ (Figure 1A), 4-fluoro-N,N-dimethylaniline $C_8H_{10}FN$ (Figure 1B), 4-methyl-N,N-dimethylaniline $C_9H_{13}N$ (Figure 1C). This particular appearance makes it possible to master their molecular architectures. At the moment, the synthesis and applications of carbosilane dendrimers are of interest. There have been reported that these carbosilane dendrimers are non-toxic and can be functional by a variety of reactions, making them candidates for drug and catalyst carriers or having unique virtual optical characteristics (Dantlgraber et al., 2002; Ponomarenko et al., 2000; Genson et al., 2005).

The aim of this work was study the structural properties of the N,N dimethylaniline substituents in the para position. Quantum chemistry calculations have been utilized to correlate the experimental results obtained from different methods (Lahmidi et al., 2017). The Density-functional theory study (DFT) method with the B3LYP correlation and hybridization function, based on 6-311G (d, p) (Frisch et al., 2016; Duque et al., 2011), has been described to calculate the thermochemical descriptors (the optimization of the geometries, the lengths and the bond angles of the molecules, the energies and the densities of the limiting molecular orbitals, electronic chemical potential, electronegativity, chemical hardness, overall softness, overall electrophilic index, global nucleophilic index, nonlinear magnetic optical properties) to compare the stability and reactivity of these molecules and to study their biological activities by potential molecular electrostatic.

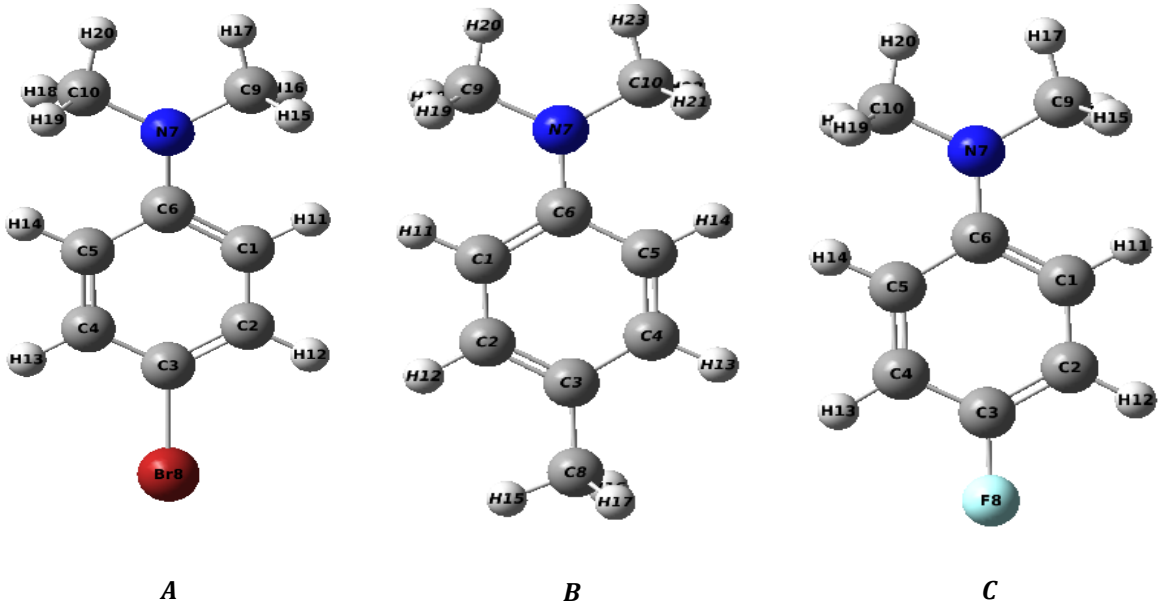

A ***B*** ***C***

Figure 1. Optimized molecular structure of (A) $C_8H_{10}BrN$, (B) $C_8H_{10}FN$, (C) $C_9H_{13}N$

2. MATERIALS AND METHODS

There are many methods of quantum chemistry such as semi-empirical methods, ab initio methods and DFT. All of these methods have the ability to determine atomic molecular properties, complex clusters, etc.

The optimized geometry of three molecules was studied by B3LYP / 6-311G (d, p) method (Sebastian et al., 2015; Liu and Gao, 2012). All the calculations in this study were used with the Gaussian 09 program. The length and angle of connection were given by the DFT method. The following quantum chemical indices have been taken into account: the energy of the highest occupied molecular orbit (E_{HOMO}), the energy of the lowest unoccupied molecular orbit (E_{LUMO}), the energy band gap $\Delta E = E_{HOMO}-E_{LUMO}$, the quantum descriptors, the electronic affinity (A), the ionization potential (I) and the atomic partial charges (Q) were calculated for the two structures from the potential electrostatic surface (ESP) according to the same theory of levels (Liu and Gao, 2012).

3. RESULTS AND DISCUSSION

3.1 Quantum chemical calculation

The essential orbitals responsible for chemical stability are the highest occupied molecular orbit (HOMO) and the lowest unoccupied molecular orbit (LUMO). The HOMO describes the capacity to produce the electrons, however, LUMO defines the capacity to gain the electrons. Electronic absorption regarding the passage of the soil in the first level of excitement defined by an electronic excitation from the HOMO to the LUMO (Kovács et al., 1999). The HOMO and LUMO of each molecule are illustrated in Figure 2. Mulliken population analysis was used to study the electronic charges on the atoms of the molecule. The Mulliken charges of the three molecules are given in Figure 3.

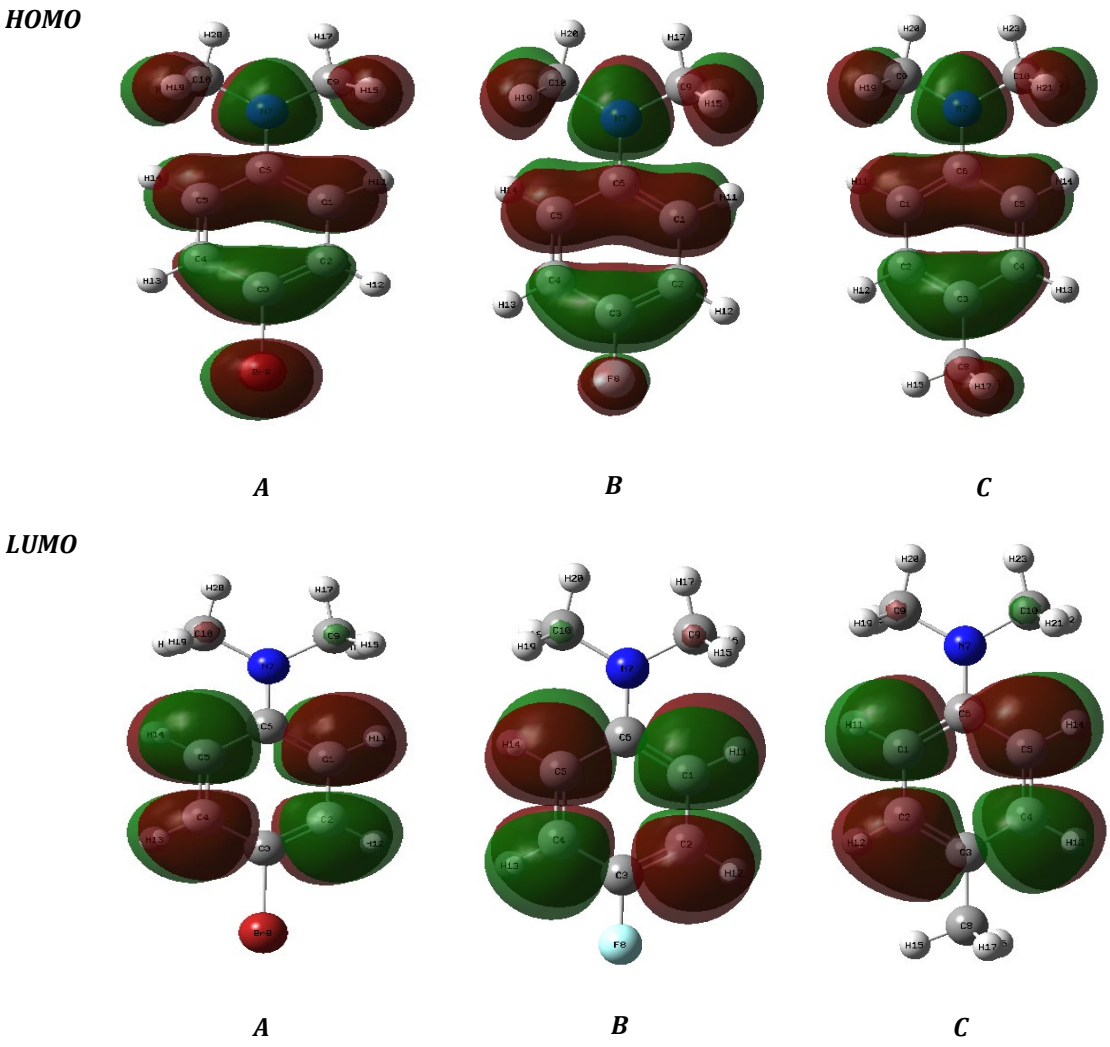

Figure 2. HOMO and LUMO of (A) $C_8H_{10}BrN$, (B) $C_8H_{10}FN$, and (C) $C_9H_{13}N$ by the DFT/B3LYP method

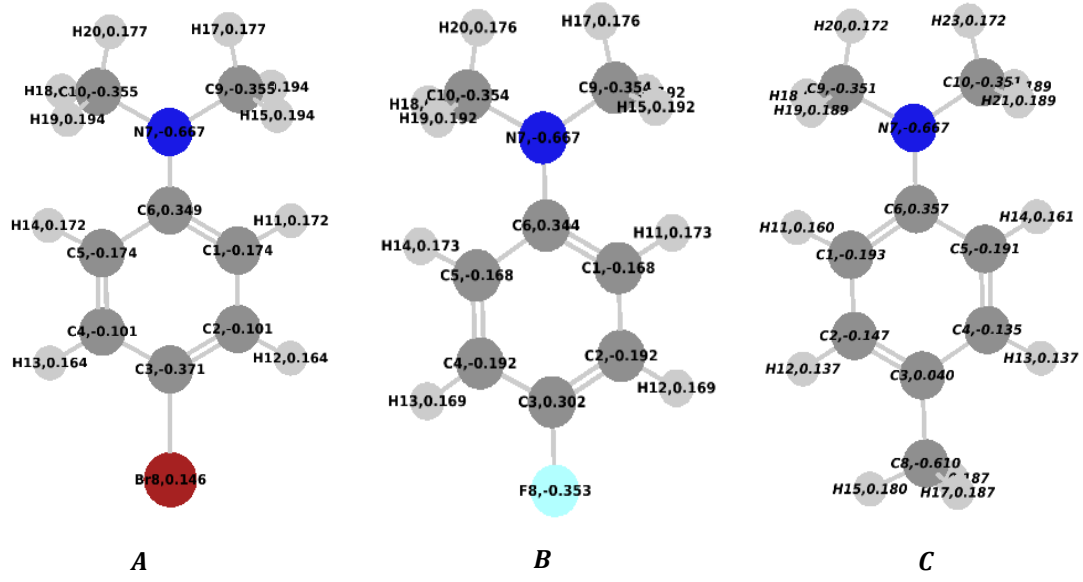

Figure 3. Mulliken charges of (A) $C_8H_{10}BrN$, (B) $C_8H_{10}FN$, and (C) $C_9H_{13}N$ by the DFT/B3LYP method

The following quantum descriptors were calculated from the optimized structure obtained: Ionization potential: $I = -E_{HOMO}$

Electronic affinity: $A = -E_{LUMO}$

Absolute electronegativity: $\chi = \frac{I+A}{2}$

Overall hardness: $\eta = I - A$

Overall softness: $\sigma = \frac{1}{\eta} = \frac{1}{E_{LUMO}-E_{HOMO}}$

Electronic chemical potential: $\mu = -\frac{(I+A)}{2}$

Maximum charge transfer: $\Delta Nmax = -\frac{\mu}{\eta}$

Overall electrophilicity: $\omega = \frac{\mu^2}{2\eta}$

Overall nucleophilia N: $N = E_{HOMO} - E_{HOMO(TCE)}$ with $E_{HOMO(TCE)}$ = -9.3686 eV calculated by DFT/B3LYP.

To get an idea of the overall reactivity of the three molecules, I, A, μ, χ, η, σ, ω, N and ΔN_{max} were calculated (Table 1).

Table 1. Quantum theoretical parameters of $C_8H_{10}BrN$, $C_8H_{10}FN$, and $C_9H_{13}N$, calculated by B3LYP / 6-311G (d, p)

Parameters	**E_{LUMO} (eV)**	**E_{HOMO} (eV)**	**ΔE (eV)**	**I (eV)**	**A (eV)**	**μ (eV)**
$C_8H_{10}BrN$	-0.3361	-5.3611	5.025	5.3611	0.3361	-2.8486
Parameters	**χ (eV)**	**η (eV)**	**σ (eV^{-1})**	**ω (eV)**	**N (eV)**	**ΔN_{max}(eV)**
$C_8H_{10}BrN$	2.8486	5.025	0.1990	0.8074	4.0075	0.5668
Parameters	**E_{LUMO} (eV)**	**E_{HOMO} (eV)**	**ΔE (eV)**	**I (eV)**	**A (eV)**	**μ (eV)**
$C_8H_{10}FN$	-0.3522	-5.3069	4.9546	5.3069	0.3522	-2.8295
Parameters	**χ (eV)**	**η (eV)**	**σ (eV^{-1})**	**ω (eV)**	**N (eV)**	**ΔN_{max}(eV)**
$C_8H_{10}FN$	2.8295	4.9547	0.2018	0.8079	4.0617	0.5710
Parameters	**E_{LUMO} (eV)**	**E_{HOMO} (eV)**	**ΔE (eV)**	**I (eV)**	**A (eV)**	**μ (eV)**
$C_9H_{13}N$	0.1120	-4.9699	5.0819	4.9699	-0.1120	-2.4289
Parameters	**χ (eV)**	**η (eV)**	**σ (eV^{-1})**	**ω (eV)**	**N (eV)**	**ΔN_{max} (eV)**
$C_9H_{13}N$	2.4289	5.0819	0.1967	0.5804	4.39	0.4779

The calculated energy gap values were 5.025 eV, 4.9546 eV, and 5.0819 eV for $C_8H_{10}BrN$, $C_8H_{10}FN$, and $C_9H_{13}N$, respectively. These values were almost similar for the three molecules. The overall electrophilicity index values were 0.8074 eV, 0.8079 eV and 0.5804 eV for $C_8H_{10}BrN$, $C_8H_{10}FN$, and $C_9H_{13}N$, respectively. As a result, the reactivity of $C_8H_{10}BrN$ and $C_8H_{10}FN$ to nucleophilic attack was greater than that of $C_9H_{13}N$. The overall nucleophilicity index values were 4.0075 eV, 4.0617 eV and 4.39 eV for $C_8H_{10}BrN$, $C_8H_{10}FN$, and $C_9H_{13}N$. This showed that the reactivity of $C_9H_{13}N$ to electrophilic attack was greater than that of $C_8H_{10}BrN$ and $C_8H_{10}FN$. The maximum charge transfer ΔN_{max} of the three molecules was almost equal to 0.5 eV.

3.2 Non-linear optical properties

Intermolecular interactions such as drugs are widely understood by dipole moment and the energetic terms of hyperpolarization of the first and second-order. The dipole moment (μ), the polarizability (α), the first hyperpolarizability (β) and the second hyperpolarizability (γ) were calculated using a basic set of DFT on the basis of the 6-311G (d, p). The complete equations to calculate the amplitude of μ, α, β and γ, using the components x, y, z of 09W Gaussian output, are as follows (Liu et al., 2012; EL Ouafy et al., 2021)

$$\mu = (\mu_x^2 + \mu_y^2 + \mu_z^2)^{1/2}$$

$$\alpha = \frac{(\alpha_{xx} + \alpha_{yy} + \alpha_{zz})}{3}$$

$$\beta = (\beta_x^2 + \beta_y^2 + \beta_z^2)^{1/2}$$

$$\beta_x = \beta_{xxx} + \beta_{xyy} + \beta_{xzz}$$

$$\beta_y = \beta_{yyy} + \beta_{xxy} + \beta_{yzz}$$

$$\beta_z = \beta_{zzz} + \beta_{xxz} + \beta_{yyz}$$

$$< \gamma > = \frac{1}{5}\left(\gamma_{xxxx} + \gamma_{yyyy} + \gamma_{zzzz} + 2\left[\gamma_{xxyy} + \gamma_{yyzz} + \gamma_{xxzz}\right]\right)$$

The results for the non-linear optical properties of molecules are shown in Table 2. The μ of the molecules was again calculated using DFT/B3LYP method with basic set 6-311G (d, p). It indicated the distribution of molecular charges and was given as a three-dimensional vector. Consequently, it can be utilized as a descriptor to represent the charge movement through the molecule as a function of the positive and negative charge centers. The μ was determined for neutral molecules. For charged molecules, its values depended on the orientation and the choice of the origin of the molecular.

The results showed that the measured value of the dipole moment of $C_8H_{10}BrN$ (4.3724 D) was greater than those of $C_8H_{10}FN$ (3.9173 D) and $C_9H_{13}N$ (1.9559 D), which reflected the slight stability of $C_8H_{10}BrN$ with respect to other molecules.

The value of the dipolar polarizability tensors of $C_8H_{10}FN$ and $C_9H_{13}N$ were high in all three directions, compared to the values of the polarizability tensors of $C_8H_{10}BrN$. The high values of the calculated dipole polarization were -59.4876 D and -59.9918 D for $C_8H_{10}FN$ and $C_9H_{13}N$, respectively, while the low value of dipolar

polarization (-69.9556 D) was observed in $C_8H_{10}BrN$. So, $C_8H_{10}FN$ and $C_9H_{13}N$ were slightly polarizable and were mildly chemically active.

The transitions of $C_8H_{10}BrN$ 38.8795 D, 0.0001 D and 0.001 D were observed along the x, y and z axes with a positive direction, whereas the transitions of $C_8H_{10}FN$ 28.9127 D, 0.0014 D and 0.0005 D were found along the x, y and z axes with a positive direction and the $C_9H_{13}N$ transitions -20.1038 D, 0.3983 D and 0.2827 D were found along the x, z and y axes. The high and low β were calculated to be 85.7714 D and 19.4117 in $C_8H_{10}BrN$ and $C_8H_{10}FN$, respectively. Therefore, electron delocalization and charge transfer increased in $C_8H_{10}BrN$, resulting in a greater β response of $C_8H_{10}BrN$, compared to other molecules.

The values of the second-order hyperpolarizability γ, as well as their contributing tensors, were also observed to be greater in $C_8H_{10}FN$, and $C_9H_{13}N$, compared to 4 $C_8H_{10}BrN$.

3.3 Thermodynamic parameters

The enthalpy ΔH, entropy ΔS and free energy ΔG were determined for each molecule (Table 3). The enthalpy is a quantity related to the energy of a thermodynamic system. It includes the internal energy of the system, to which is added the product of the pressure by the volume. ΔS was characterized by the degree of disorder or unpredictability of the information contained in a system. ΔG of $C_8H_{10}BrN$ was lower than $C_8H_{10}FN$ and $C_9H_{13}N$. This result meant that $C_8H_{10}BrN$ was thermodynamically more stable than other molecules.

Table 2. Electric dipole moments (Debye) by the DFT method of $C_8H_{10}BrN$, $C_8H_{10}FN$, and $C_9H_{13}N$ calculated by B3LYP / 6-311G (d, p)

	Parameters	$C_8H_{10}BrN$	$C_8H_{10}FN$	$C_9H_{13}N$
Dipole moment (Debye)	μ_x	-4.3724	3.9173	-1.9550
	μ_y	0.0001	0.0002	-0.0580
	μ_z	0.0000	-0.0003	0.0132
	μ	4.3724	3.9173	1.9559
Polarizability (Debye)	α_{xx}	-66.0092	-62.4819	-56.7768
	α_{yy}	-67.2151	-53.5739	-57.6945
	α_{zz}	-76.6425	-62.4071	-65.5043
	α	-69.9556	-59.4876	-59.9918
First Hyperpolarizability (Debye)	β_{xxx}	38.8795	28.9127	-20.1038
	β_{xyy}	20.4812	-6.2653	-4.1796
	β_{xzz}	26.4107	-3.2327	-5.9507
	β_{yyy}	0.0001	0.0014	0.2827
	β_{xxy}	0.0029	0.0018	-0.1713
	β_{yzz}	0.0008	-0.0002	-0.5204
	β_{zzz}	0.0010	0.0005	0.3983
	β_{xxz}	0.0024	-0.0019	0.0281
	β_{yyz}	-0.0008	-0.0012	-0.3466
	β	85.7714	19.4147	30.2369
Second Hyperpolarizability (Debye)	γ_{xxxx}	-2673.2074	-1630.8691	-1816.7288
	γ_{yyyy}	-450.3040	-432.2042	-455.1513
	γ_{zzzz}	-140.7362	-120.2242	-134.0489
	γ_{xxyy}	-528.8154	-308.6378	-365.0172
	γ_{yyzz}	-105.6279	-99.3631	-104.6965
	γ_{xxzz}	-495.2935	-269.0021	-321.7364
	γ	-1104.7442	-671.4607	-797.7656

Table 3. Thermodynamic parameters of $C_8H_{10}BrN$, $C_8H_{10}FN$, and $C_9H_{13}N$

Molecules	ΔH° (kcal/mol)	ΔS° (kcal/mol/K)	ΔG° (kcal/mol)
$C_8H_{10}BrN$	-291960.94	0.0857	-291989.45
$C_8H_{10}FN$	-254331.08	0.0964	-254359.81
$C_9H_{13}N$	-184455.55	0.1010	-214553.55

3.4 Bond length and angle properties

The DFT level has been used with the B3LYP/6-311G (d, p) ; method, the utility of which is to describe the molecular physical and chemical properties (Gasteiger et al., 1994).

Tables 4 and 5 show the comparison of the optimized bond length and the angle between experimental and calculated atomic numbered positions (Figure 1). The optimized structure using a periodic DFT calculation

corresponded exactly to an experimental result. The study of the geometric product, therefore, showed an excellent agreement between theoretical and experimental results.

3.5 Molecular electrostatic potential

Molecular electrostatic potential (MEP) results determine regions of electrophilic or nucleophilic attack (Hathwar et al., 2010). The MEP is mainly used in the form of the reactivity map showing the region's most likely for the electrophilic attack of molecules. Contour MEP and the map produce a tool for predicting how different geometries may interact. The total electron density and the MEP surface of the molecules studied were obtained by B3LYP / 6-311G (d, p). Electrostatic potential maps and contour electrostatic potential of $C_8H_{10}BrN$, $C_8H_{10}FN$, and $C_9H_{13}N$ are given in Figures 4 and 5. The red-colored parts of the MEP surface are rich in electrons; blue is electron deficient; light blue is slightly electron deficient; yellow is slightly rich in electrons; green is neutral. The positively charged regions indicate the nucleophilic attack parts while the red-colored parts indicate the regions intended for the electrophilic attack. The sites of electrophilic attack were Br8, F8 and N7 for $C_8H_{10}BrN$, $C_8H_{10}FN$ and $C_9H_{13}N$, respectively.

Table 4. Bond lengths (Å) of $C_8H_{10}BrN$, $C_8H_{10}FN$, and $C_9H_{13}N$

Bond length (Å)	$C_8H_{10}BrN$	$C_8H_{10}FN$	$C_9H_{13}N$	Exp 4-methylaniline
C1-C2	1.3948	1.3948	1.3948	1.40
C2-C3	1.3949	1.3949	1.3949	1.39
C3-C4	1.3948	1.3948	1.3948	1.36
C4-C5	1.3948	1.3948	1.3948	1.39
C5-C6	1.3949	1.3949	1.3949	1.39
C6-N7	1.266	1.266	1.266	---
N7-C9	1.4699	1.4701	1.47	1.43
N7-C10	1.4701	1.47	1.4701	1.40
C3-Br8	1.881	---	---	---
C3-F8	---	1.32	---	---
C3-C8	---	---	1.4969	1.55

Note: The experimental values of the first were extracted from the crystal structure (Tzeng et al., 1998)

Table 5. Angles (θº) of $C_8H_{10}BrN$, $C_8H_{10}FN$, and $C_9H_{13}N$

Angles (θº)	$C_8H_{10}BrN$	$C_8H_{10}FN$	$C_9H_{13}N$	Exp 4-methylaniline
C1-C2-C3	120.0007	119.9969	119.9969	120.5
C2-C3-C4	120.0002	120.0002	120.0002	120.5
C3-C4-C5	120.0033	120.0018	120.0033	120.3
C5-C6-N7	119.9954	120.0009	120.0033	---
C9-N7-C10	120.0034	119.9994	119.9993	119.2
C2-C3-Br8	119.9997	---	---	---
C2-C3-F8	---	119.9984	---	---
C2-C3-C8	---	---	119.9992	119.2

Note: The experimental values of the first are extracted from the crystal structure (Tzeng et al., 1998)

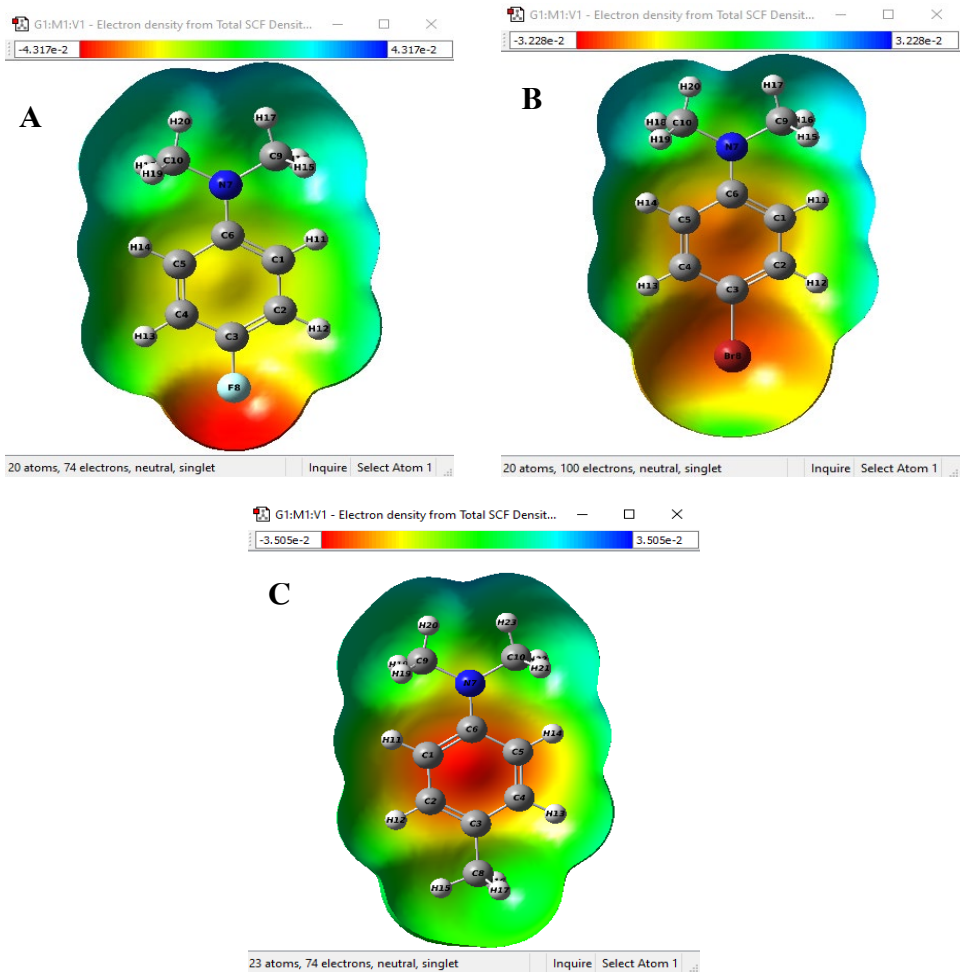

Figure 4. Electrostatic potential maps around the molecule of (A) $C_8H_{10}BrN$, (B) $C_8H_{10}FN$, and (C) $C_9H_{13}N$

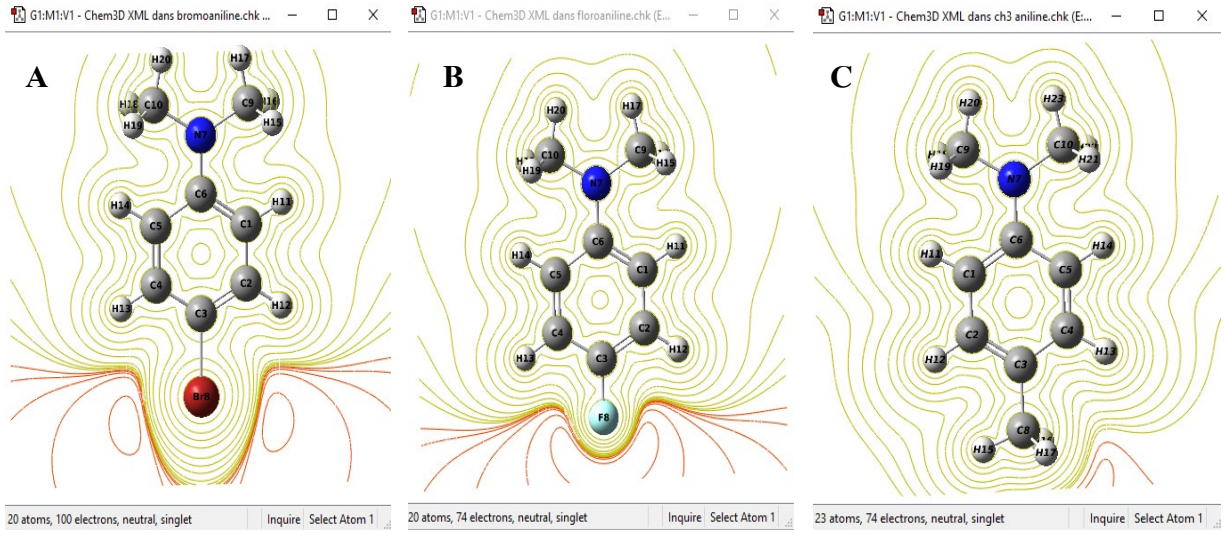

Figure 5. Contour electrostatic potential around the molecule of conformers of (A) $C_8H_{10}BrN$, (B) $C_8H_{10}FN$, and (C) $C_9H_{13}N$

4. CONCLUSION

The electronic properties of $C_8H_{10}BrN$, $C_8H_{10}FN$ and $C_9H_{13}N$ were calculated. The HOMO and LUMO energy deviations described the possible charge, transfer interactions taking place in the molecules, the determination of the theoretical molecular structures, the electrostatic potential contour and electrostatic potential maps around molecules have been found by the DFT method using the B3LYP / 6-311G (d, p) basis. The MEP surface can lead to an understanding of the properties and activity of molecules. Linear polarizability (α), first hyperpolarizability (β) and second hyperpolarizability (γ) values of the studied molecule were calculated.

In summary, some important points could be concluded. DFT/B3LYP/6-311G (d, p) has been found to be a good computational method to predict the geometric results. Global descriptors, thermodynamic study and nonlinear optical properties have shown that $C_9H_{13}N$ was more reactive (HOMO and LUMO were close to each other) and $C_8H_{10}BrN$ is the stable molecule. The electrostatic potential molecule motivated the regions rich in electrons intended for electrophilic attacks as well as the positive electron acceptor sites.

REFERENCES

EL Ouafy, H., EL Ouafy, T., Oubenali, M., EL Haimouti, A., Gamouh, A., and Mbarki, M. (2021). Analysis of the chemical reactivity of limonene by the functional density theory method using global descriptors. *Journal of Chemical Health Risks,* 11(2), 213-221.

Dantlgraber, G., Baumeister, U., Diele, S., Kresse, H., Lühmann, B., Lang, H., and Tschierske, C. (2002). Preuve d'une nouvelle phase cristalline liquide à commutation ferroélectrique formée par un dendrimère à base de carbosilane avec des unités mésogènes en forme de banane. *Journal de l'American Chemical Society*, 124 (50), 14852-14853.

Duque, A. F., Bessa, V. S., Carvalho, M. F., and Castro, P. M. L., (2011). Bioaugmentation of a rotating biological contactor for degradation of 2-fluorophenol. *Bioresource Technology*. 102(19), 9300-9303.

Frisch, M. J., Trucks, G. W., Schlegel, H. B., Scuseria, G. E., Robb, M. A., Cheeseman, J. R., Scalmani, G., Barone, V., Patersson, G. A., Nakatsuji, H., Li, X., Caricato, M., Marenich, A., Bloino, J., Kenesko, B. G., Gomperts, R., Mennucci, B., Hratchian, H. P., Ortiz, J. V., . . . Fox, D. J. (2016). Gaussian 09, Revision A.02. Inc., Wallingford CT. *Expanding the limits of computational chemistry*, [Online URL: https://gaussian.com/g09citation/] accessed on November 10, 2020.

Genson, K. L., Holzmueller, J., Leshchiner, I., Agina, E., Boiko, N., Shibaev, V. P., and Tsukruk, V. V. (2005). Organized monolayers of carbosilane dendrimers with mesogenic terminalgroups. *Macromolecules*, 38(19), 8028-8035.

Hathwar, V. R., Pal, R., and Guru Row, T. N. (2010). Charge density analysis of crystals of nicotinamide with salicylic acid and oxalic acid: an insight into the salt to cocrystal continuum. *Crystal Growth and Design*, 10(8), 3306-3310.

Kovács, A., Macsári, I., and Hargittai, I. (1999). Intramolecular hydrogen bonding in fluorophenol derivatives: 2-fluorophenol, 2, 6-difluorophenol, and 2, 3, 5, 6-tetrafluorohydroquinone. *The Journal of Physical Chemistry A*, 103(16), 3110-3114.

Lahmidi, S., Elyoussfi, A., Dafali, A., Elmsellem, H., Sebbar, N. K., El Ouasif, L., and Hammouti, B. (2017). Corrosion inhibition of mild steel by two new 1, 2, 4-triazolo [1, 5-a] pyrimidine derivatives in 1 M HCl: Experimental and computational study. *Journal of Materials and Environmental Science*, 8, 225-237.

Liu, L., and Gao, H. (2012). Molecular structure and vibrational spectra of ibuprofen using density function theory calculations. *Spectrochimica Acta Part A: Molecular and Biomolecular Spectroscopy*, 89, 201-209.

Gasteiger, J., Li, X., Rudolph, C., Sadowski, J., and Zupan, J. (1994). Representation of molecular electrostatic potentials by topological feature maps. *Journal of the American Chemical Society*. 116(11), 4608-4620.

Pardo, R., Zayat, M., and Levy, D. (2011). Photochromic organic–inorganic hybrid materials. *Chemical Society Reviews*, 40(2), 672-687.

Ponomarenko, S. A., Boiko, N. I., Shibaev, V. P., and Magonov, S. N. (2000). Atomic force microscopy study of structural organization of carbosilane liquid crystalline dendrimer. *Langmuir*, 16(12), 5487-5493.

Sebastian, S., Sylvestre, S., Jayabharathi, J., Ayyapan, S., Amalanathan, M., Oudayakumar, K., and Herman, I. A. (2015). Study on conformational stability, molecular structure, vibrational spectra, NBO, TD-DFT, HOMO and LUMO analysis of 3, 5-dinitrosalicylic acid by DFT techniques. *Spectrochimica Acta Part A: Molecular and Biomolecular Spectroscopy*, 136, 1107-1118.

Tzeng, W. B, Narayanan, K., Shieh, K. C., and Tung, C. C. (1998). A study of the structures and vibrations of $C_6H_5NH_2$, C_6H_5NHD, $C_6H_5ND_2$, in the state S1 by calculations Ab Initio. *Journal of Molecular Structure: THEOCHEM*, 428(1-3), 231-240.

Wojtaś, M., Ga, A., Czupiński, O., Pietraszko, A., and Jakubas, R. (2009). Perchlorate de 2, 4, 6-triméthylpyridinium : propriétés polaires et corrélations avec la structure moléculaire du cristal hybride organique-inorganique. *Journal of Solid State Chemistry*, 182 (11), 3021-3030.